



ELSEVIER

Available online at [www.sciencedirect.com](http://www.sciencedirect.com)

ScienceDirect

Proceedings of the Combustion Institute 000 (2016) 1–7

Proceedings  
of the  
Combustion  
Institute[www.elsevier.com/locate/proci](http://www.elsevier.com/locate/proci)

# Instantaneous 3D imaging of flame species using coded laser illumination

Elias Kristensson\*, Zheming Li, Edouard Berrocal, Mattias Richter,  
Marcus Aldén

*Division of combustion Physics, Lund University, Professorsgatan 1, S-223 63 Box 118, Lund 221 00, Sweden*

Received 1 December 2015; accepted 13 August 2016

Available online xxx

## Abstract

Three-dimensional (3D) imaging of dynamic objects that rapidly undergoes structural changes, such as turbulent combusting flows, has been a long-standing challenge, mainly due to the common need for sequential image acquisitions. To accurately sense the 3D shape of the sample, all acquisitions need to be recorded within a sufficiently short time-scale during which the sample appears stationary. Here we present a versatile diagnostic method, named Frequency Recognition Algorithm for Multiple Exposures (FRAME) that enables instantaneous 3D imaging. FRAME is based on volumetric laser sheet imaging but permits several layers to be probed parallel in time and acquired using a single detector. To differentiate between the signals arising from the different layers FRAME incorporates a line-coding strategy, in which each laser sheet is given a unique spatial intensity modulation. Although the signal from all laser sheets overlap in the spatial domain, this line-coding approach makes them separated in the frequency domain where they can be accessed individually by means of digital filtering. Here we demonstrate this method by studying laser-induced fluorescence from formaldehyde in a flame and present 3D images of the flame topology, instantaneously acquired.

© 2016 by The Combustion Institute. Published by Elsevier Inc.

*Keywords:* Three-dimensional imaging; Structured illumination; Instantaneous imaging; Coded imaging

## 1. Introduction

Sensing the three-dimensional (3D) shape of a sample via optical means is of scientific importance in many fields and one can find different techniques capable of this in the literature. Some are designed primarily for solid samples, such as holography [1] and fringe projection [2] whereas

others are better suited for semi-transparent objects, including tomography [3,4], volumetric laser sheet imaging [5–9] and structured illumination scanning [10]. Semi-transparent objects often require a scanning procedure, where e.g. different layers of the sample are probed sequentially. Consequently, assessing the 3D nature of a semi-transparent object that, in addition, undergoes rapid structural changes becomes a challenging task and several methods have been developed to address this issue. By using a cluster of laser sources together with a multi-frame ICCD camera such a semi-transparent sample can be rapidly scanned

\* Corresponding author. Fax: +46 46 222 45 42.

E-mail address: [elias.kristensson@forbrf.lth.se](mailto:elias.kristensson@forbrf.lth.se) (E. Kristensson).

<http://dx.doi.org/10.1016/j.proci.2016.08.040>

1540-7489 © 2016 by The Combustion Institute. Published by Elsevier Inc.

(within  $\sim 50 \mu\text{s}$ ) and 3D images constructed from 8 laser sheet images of combustion events have been presented using this approach [7,8]. Mantzaras et al. employed a multi-color illumination scheme to visualize four layers of a combusting flow parallel in time, from which the 3D structure of the sample could be reconstructed [11]. The approach relied, however, on Mie scattering, thus restricting the technique to imaging of particulates. Wellander et al. developed a 4D imaging system based on rapidly sweeping several laser sheets across the object, delivering 3D videos at 1 kHz [5]. By combining a high-speed laser system with a polygonal laser scanner unit, Weinkauff et al. also achieved time-resolved 3D imaging in the kHz regime [9]. The advent of mega-hertz pulse burst laser systems has opened up for 3D imaging at even greater frame rates [12–14].

In this paper, we present a versatile diagnostic technique called Frequency Recognition Algorithm for Multiple Exposures (FRAME) that permits snapshot 3D imaging using coded illumination and we believe FRAME constitutes an attractive new alternative for imaging of rapid, dynamic events, such as turbulent flames.

## 2. Frequency recognition algorithm for multiple exposures (FRAME)

During the last decade the performance of 2D detectors has improved significantly and sensitive mega-pixel sensors with up to 16-bits dynamic range are standard laboratory equipment nowadays. However, in many imaging applications the full capacity of these detectors is not exploited. For example, in the field of astrophotography the numerical aperture of the collection optics is unavoidably very low, directly limiting spatial resolution. In the field of tissue imaging (or other scattering media), the sample inherently acts as a low-pass filter. In combustion research, diffusion has a smoothing effect that reduces contrast. Users with applications relying on image intensification discover a loss of fine structures due to the conversion between photons and electrons. Hence, employing a high-resolution detector does not always lead to a high-resolution image. The FRAME methodology takes advantage of this fact in order to permit a single detector to acquire and store several images simultaneously on-chip.

Traditionally, a camera sensor needs to be read and reset before it can be re-exposed to light. FRAME circumvents this need by employing “coded illumination”, where each laser sheet is given a unique imprint. Technically, the intensity profile of each laser sheet is modulated with a sinusoidal pattern with a frequency of  $\nu$  and an amplitude of  $m$ . As the light interacts with the sample, this structured field and the sample structures ( $A$ )

are superposed multiplicatively, according to:

$$I_{\text{mod}} = A \cdot (1 + m \sin(\nu \cdot x)) \quad (1)$$

The outcome,  $I_{\text{mod}}$ , thus contains three “copies” of  $A$  in the Fourier domain (reciprocal space); one centered at the origin and two centered at  $\pm\nu$ . By altering this spatial frequency, the image copies are transferred either closer to or farther away from the origin, thus granting access to the otherwise (often) unexploited high spatial frequency regions of a detector. By giving laser sheets different  $\nu$ , their respective sample structures become transferred into different offset locations in reciprocal space, where they can be accessed individually in the data post-processing using 2D lock-in detection algorithms [15,16]. However, by varying the modulation frequency alone, the two-dimensionality of the detector is not fully exploited and to take full advantage of the second spatial dimension one should also alter the angular component of the modulation, achieved by simply changing the angle of incidence for the laser sheets. This feature increases the bandwidth, i.e. the image-storing capacity, considerably.

The FRAME concept is illustrated in Fig. 1 where a coded field illuminates a sample that is characterized primarily by low spatial frequencies (i.e. weak gradients). Most of the sample information is thus condensed near the origin in the center of the Fourier domain (see Fig. 1a) – the remaining space is mostly void. Image copies of such a sample can thus be strategically placed at different locations in the vacant high frequency regions. If each modulation is unique (in terms of frequency and/or orientation), there will be an insignificant crosstalk between the copies, see Fig. 1d.

Unmixing the acquired data to access each image copy individually is accomplished using a frequency-sensitive demodulation algorithm. In the procedure, each image copy is first isolated in reciprocal space by means of a digital 2D band-pass filter, effectively removing all other image copies temporarily. The isolated data is then digitally transferred to the center of the Fourier domain, a process that turns modulation amplitude into a non-modulated dc-component. Applying the inverse Fourier transform on this filtered and rearranged dataset turns the spatial frequencies from the offset location in reciprocal space into intensity values, thus revealing the image information stored there.

Figure 2 shows an example of a FRAME measurement where a glass cuvette with a fluorescing dye is probed with two differently coded laser sheets being separated by a distance of 4 mm, thereby probing slightly different sections of the sample. Inserted into the cuvette is a thin metal piece that, in Fig. 2a, is positioned in front of both sheets. Although the signal from both laser sheets overlap in space on the detector, their different modulation features transfer their sample structures

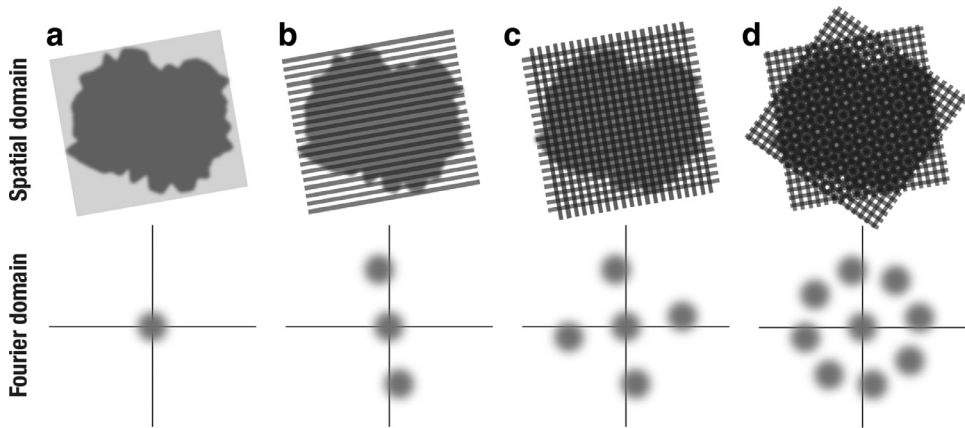


Fig. 1. The FRAME concept. (a) Uniform illumination of a sample that is described primarily by low spatial frequencies. (b) Illumination using intensity modulation, which effectively places two “copies” of the sample structures in otherwise unused space in the Fourier domain. (c)–(d) Examples of multiple-illumination schemes.

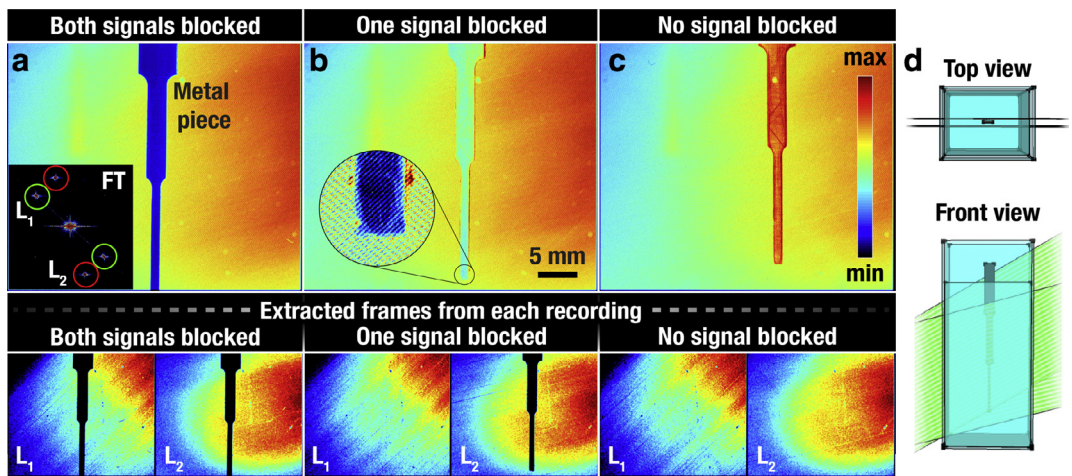


Fig. 2. A FRAME measurement, where a cuvette with dye is probed using two differently coded laser sheets at two medial positions. A metal piece is positioned (a) in front of-, (b) between- and (c) behind the laser sheets. The Fourier transform of the image in (a) is provided in the inset, wherein the 2D band-pass filters employed to extract the “image copies” are marked. The outcome of the FRAME analysis of each image is given below each individual case, marked as either  $L_1$  or  $L_2$ . (d) Schematic illustrations of the sample in case (b). Note that the intensity in the magnified region in (b) is adjusted to highlight the superimposed high frequency modulation.

to different positions in the Fourier domain (see inset) where they are accessed individually using the frequency-sensitive algorithm. The extracted frames both show, as expected, a shadow of the obstruction. In Fig. 2b the metal piece is positioned in-between the laser sheets and the analyzed data clearly shows how FRAME is capable of separating the two signal components. In the final example, Fig. 2c, the obstruction is placed behind both sheets and therefore not expected to affect the measurement. However, despite being placed out-of-view, the metal piece appears in the raw data image, which is due to light being reflected upon its surface. Such indirect signal contributions will, however, not carry the line-coding information super-

imposed on the laser sheet profiles and is therefore filtered out in the data post-processing, as seen in the extracted frames. This example thus illustrates that apart from being able to acquire more than one image per acquisition, FRAME also inherits the filtering capabilities associated with structured illumination [17].

### 3. Experimental setup

In order to test the FRAME methodology for instantaneous 3D imaging, four pulsed Nd:YAG lasers were employed, each operating at  $\lambda = 355$  nm and with a repetition rate of 10 Hz, delivering

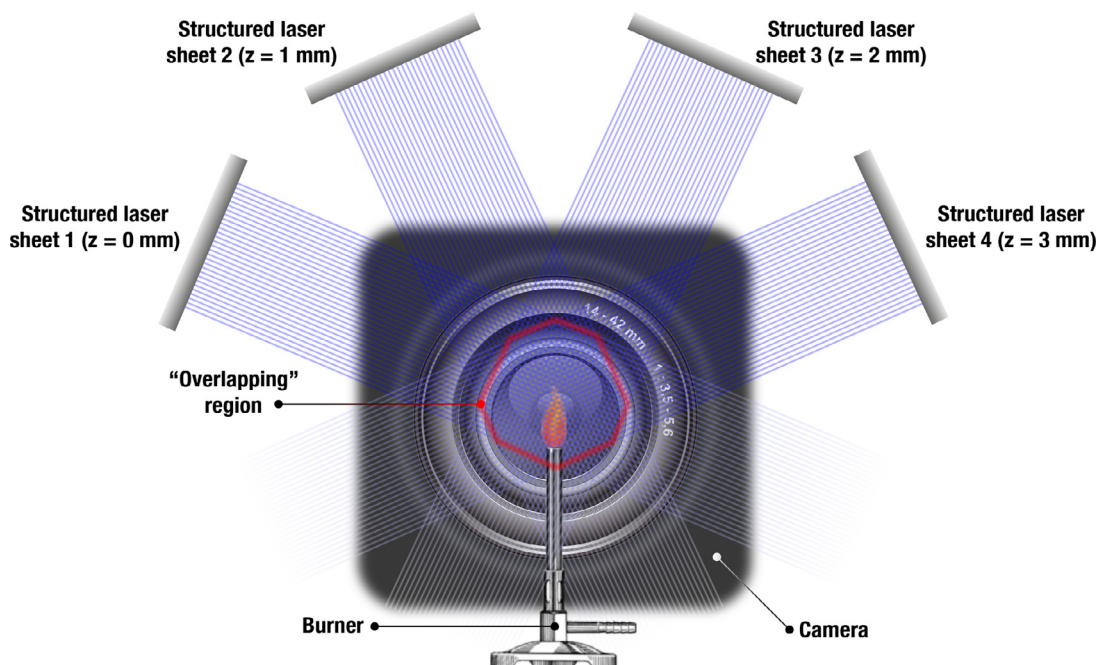


Fig. 3. Schematic of the optical configuration. The four structured laser sheets arrive at different angles (approximately  $20^\circ$ ,  $65^\circ$ ,  $115^\circ$ ,  $160^\circ$ ), effectively placing the respective signals at different locations in reciprocal space. The spatial frequency of the superimposed intensity modulation was approximately 5 lp/mm.

approximately 300 mJ per pulse. Before being guided through the sheet-forming optics, each laser was first directed through a 2" transmission grating (10 lp/mm), which added the necessary line structure to the intensity profile. This periodic structure was then imaged onto the sample whilst simultaneously focusing the laser into a thin ( $\sim 100 \mu\text{m}$ ), slightly diverging sheet (focal length: 1000 mm). Optical periscopes were utilized to alter the angle of incidence as well as to fix the sheet separation of 1 mm along the depth direction, thus setting the depth resolution. Decreasing the sheet separation provides better depth resolution, yet it reduces the field-of-view along the depth direction. During the study a Bunsen-like burner was probed and the laser-induced fluorescence (LIF) from formaldehyde molecules was collected using an ICCD camera (PI-MAX3), having an exposure time of 50 ns. To maintain focus throughout the entire probe volume – an essentiality for all 3D imaging techniques – the  $f$ -number of the camera objective needs to be set relatively high,  $f/8$  was used throughout the current study. Figure 3 shows the burner being irradiated with the structured laser sheets, each arriving simultaneously in time but with different angles. To suppress laser radiation, the camera was equipped with a Schott GG385 long-pass filter.

#### 4. Results and discussion

Figure 4 shows an overview of the results of the experiment. The left column presents the raw, unprocessed snapshot images wherein the signals from all laser sheets overlap spatially (on the detector). Each image is processed using the FRAME algorithm, which extracts each layer individually (middle column). Knowing the distance between each laser sheet (1 mm) permits us to reconstruct the 3D structure of the sample (right column). The 3D reconstruction process, which is described in [7], is based on displaying iso-surfaces of different values in conjunction with a shape-based interpolation scheme to create new surfaces in between the original image planes.

The need for 3D visualization when studying complex flow structures becomes clear in the presented results. Turbulence and instabilities causes the flame to wrinkle and sometimes form isolated structures that are easily identified when having access to the 3D view. Moreover, by circumventing the sequential scanning process that often is required, uncertainties caused by sample motion occurring in-between exposures are fully avoided. This becomes an important feature when studying rapid events, such as turbulent flows, where the sample may undergo structural changes on a time-scale similar to, or faster than, the scanning speed.

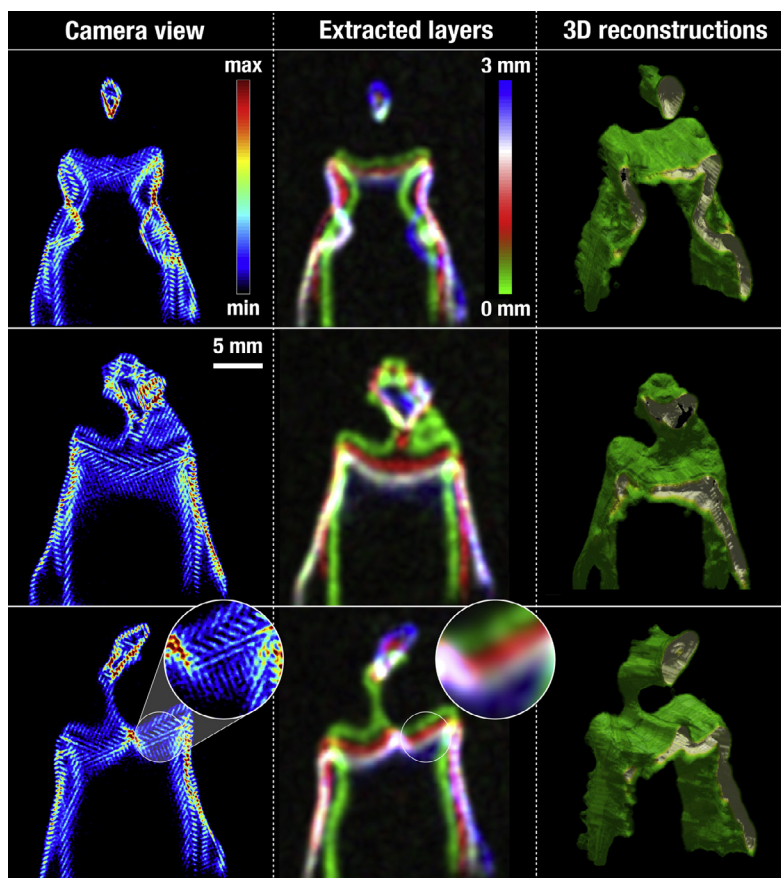


Fig. 4. (Left) Three snapshot images where the fluorescence signals from four differently coded laser sheets are super-imposed. (Middle) Data processed using the FRAME algorithm, where the extracted layers are color-coded. (Right) 3D reconstructions of the acquired data.

As described, FRAME relies on a tradeoff between image resolution and the ability to acquire several images simultaneously on a single sensor, where low-resolution images are placed in the high spatial frequency regions. These images are transferred away from the origin in reciprocal space by means of intensity modulation; the choice of modulation frequencies is therefore not an arbitrary one as it affects (1) the image-storing capacity, (2) the potential for signal crosstalk and (3) the spatial resolution of the extracted frames. Theoretically, high modulation frequencies are beneficial; as the modulation frequency for each laser sheet increases, the respective image copies are shifted farther away from the origin in reciprocal space where they are more sparsely distributed, leaving room for additional image copies. A greater separation between image copies is also needed to avoid signal crosstalk. If the image copies are packed too densely in the Fourier domain there is a risk that sample structures from one image “bleed over” into neighboring ones. Reducing the dimension of the

band-pass filter, to select only sample structures modulated at the specified spatial frequency, improves the specificity of the data extraction but can lead to a reduced spatial resolution. Figure 5 illustrates the tradeoff between specificity and spatial resolution.

In the example, the unprocessed data is presented in Fig. 5a, containing signal components from all four laser sheets. This image is then analyzed (Fig. 5b–g) using the FRAME algorithm with six different filter bandwidths, all described by 2D super-Gauss window [18]. Case (e) shows the filter settings used for the results presented in Fig. 4. The example shows that a narrow filter gives a reduced spatial resolution yet provides high selectivity with negligible signal crosstalk. The opposite occurs with a wide filter; neighboring image copies give an interfering signal contribution, while sample structures are relatively well resolved. This tradeoff between spatial resolution and signal crosstalk is optimized when FRAME is operated at the highest possible modulation frequencies

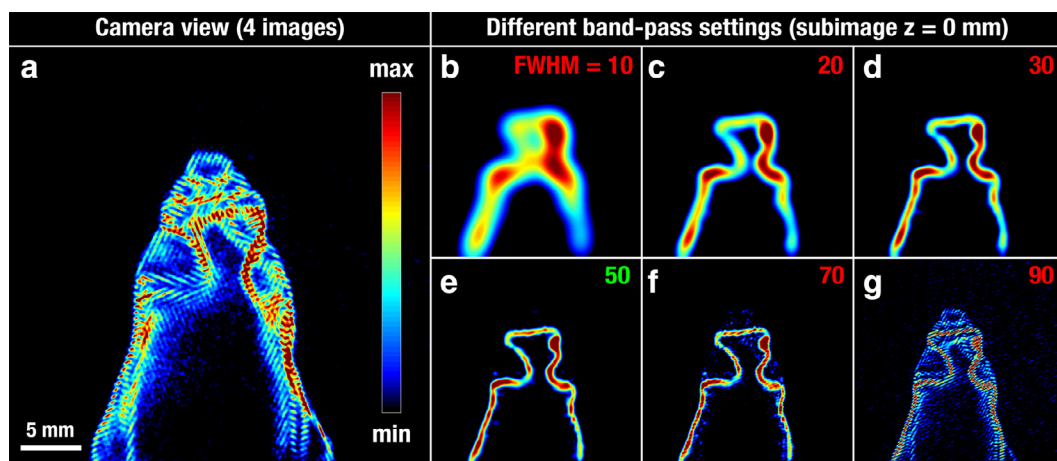


Fig. 5. Example showing the tradeoff between selectivity and spatial resolution. (a) The camera view. (b)–(g) One of the four image copies, extracted using different band-pass filters in the Fourier domain, the FWHM of the filter kernel is specified (in pixels) in each panel. Case (e) corresponds to the setting used for the results presented in the current study.

for the detection system at hand in order to optimally spread the image copies in reciprocal space. It is recommended to deduce this resolution limit of the imaging system through the modulation transfer function (MTF) [19] – estimated e.g. by analyzing the acquired spatial frequency contents of an image of a resolution target – as calculations based entirely on the pixel resolution could be misleading. Although, apart from modulation frequency, the end spatial resolution for the individual frames is also affected by several additional factors such as (1) the shape and bandwidth of the filter function, (2) the number of frames stored simultaneously on chip, (3) the type of detector (intensified cameras, for example, degrade image quality) and (4) signal-to-noise (SNR) conditions. For the current field-of-view, modulation frequency and SNR conditions, the lateral spatial resolution of the results in Fig. 4 is approximately 0.5 mm. Although, note that improvements in e.g. the MTF, pixel resolution or SNR (currently  $\sim 30$ ) should result in an improvement in spatial resolution.

In the current study the image-storing capability of FRAME was demonstrated using four laser sheet images, although it is anticipated that modern high-resolution detectors may hold a greater number of recordings simultaneously on-chip and also that this capability will increase as detector resolution improves in the future. In the present study only a few percentages of the space available in the Fourier domain were exploited, shared by (1) the image copies, together occupying  $\sim 1\%$  of the space, (2) the center peak containing most of the structural information, also filling  $\sim 1\%$  of the space and (3) empty gaps in-between the image copies to avoid signal crosstalk, taking  $\sim 1\text{--}2\%$  of the space. Figure 6 shows this current distri-

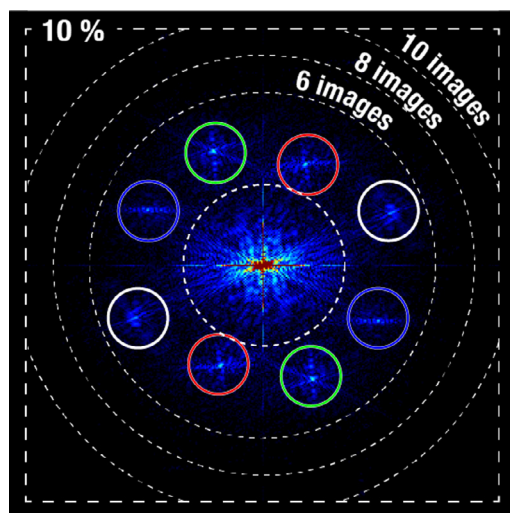


Fig. 6. 2D Fourier transform of the data shown in Fig. 5, showing how the spatial frequencies of the data are distributed. The example also shows how the image-storing capacity could be increased up to 6, 8 or 10 images by shifting the image copies farther from the origin. Note that only 10% of the Fourier domain is presented to avoid displaying void space.

bution of image data in the Fourier domain (only 10% of the Fourier domain is shown), where the inner circle marks the spread of the center peak (low spatial frequencies) and the colored circles indicate the band-pass filters. The figure also illustrates how the image-storing capacity could be improved by evenly distributing image copies of additional laser sheet images at certain distances from the origin at

slightly higher spatial frequencies. These calculated values are based on the current measurement conditions, including the necessary gap in-between image copies as well as the size of the band-pass filter currently employed. It is, however, important to mention that adding additional laser sheets to the experiment also adds complexity to the setup since each laser may require a unique optical arrangement.

## 5. Summary

In summary, a novel imaging technique called FRAME, capable of probing several layers of the sample parallel in time with a single camera, has been presented and experimentally demonstrated for instantaneous 3D laser sheet imaging of the formaldehyde distribution in a flame. Four individual lasers were employed in the current demonstration – one for each layer in the sample – but could, in principle, be replaced by a single laser source whose emission is split into several beams, granted that the laser energy is sufficient. FRAME incorporates a light-coding strategy to differentiate between different laser sheet signals, placing low-resolution versions of each image at the unexploited high frequency regions of the detector. These images are then accessed in the data post-processing via a frequency-sensitive spatial lock-in algorithm. Since all laser sheet images are stored simultaneously on-chip, the traditional need to read and reset the detector in-between successive recordings is circumvented, which opens up for data acquisition rates far beyond those originally permitted by the detection system. Finally, although the signal components in FRAME are modulated in space, the technique is governed by the same fundamental rules governing “traditional” fluorescence imaging and can thus be combined with already established methods for e.g. quantitative imaging.

## Acknowledgments

The authors wish to show their appreciation to the Swedish Energy Agency and the Knut and Alice Wallenberg Foundation for financial

support. Funding from the European Research Council (ERC) through both the Advanced Grant “TUCLA” (grant no. 669466) and the Starting Grant “Spray-Imaging” (grant no. 638546) projects are also highly appreciated.

## References

- [1] Y. Frauel, T.J. Naughton, O. Matoba, E. Tajahuerce, B. Javidi, *Proc. IEEE* 94 (2006) 636–653.
- [2] X.Y. Su, Q.C. Zhang, *Opt. Lasers Eng.* 48 (2010) 191–204.
- [3] T.D. Fansler, S.E. Parrish, *Meas. Sci. Technol.* 26 (2015).
- [4] N.A. Worth, J.R. Dawson, *Meas. Sci. Technol.* 24 (2013).
- [5] R. Wellander, M. Richter, M. Alden, *Opt. Express* 19 (2011) 21508–21514.
- [6] E.H.K. Stelzer, *Nat. Methods* 12 (2015) 23–26.
- [7] J. Nygren, J. Hult, M. Richter, et al., *Proc. Combust. Inst.* 29 (2002) 679–685.
- [8] J. Olofsson, M. Richter, M. Alden, M. Auge, *Rev. Sci. Instrum.* 77 (2006) 013104 (6 pp).
- [9] J. Weinkauff, M. Greifenstein, A. Dreizler, B. Bohm, *Meas. Sci. Technol.* 26 (2015) 105201 (15 pp).
- [10] L. Schermelleh, P.M. Carlton, S. Haase, et al., *Science* 320 (2008) 1332–1336.
- [11] J. Mantzaras, P.G. Felton, F.V. Bracco, *Three-Dimensional Visualization of Premixed-Charge Engine Flames: Islands of Reactants and Products; Fractal Dimensions; and Homogeneity*, SAE International, Warrendale, Pa, 1988.
- [12] V. Sick, *Proc. Combust. Inst* 34 (2013) 3509–3530.
- [13] R.A. Patton, K.N. Gabet, N. Jiang, W.R. Lempert, J.A. Sutton, *Appl. Phys. B-Lasers Opt.* 106 (2012) 457–471.
- [14] K.N. Gabet, R.A. Patton, N. Jiang, W.R. Lempert, J.A. Sutton, *Appl. Phys. B-Lasers Opt.* 106 (2012) 569–575.
- [15] E. Kristensson, A. Ehn, J. Bood, M. Alden, *Proc. Combust. Inst.* 35 (2015) 3689–3696.
- [16] K. Larsson, M. Jonsson, J. Borggren, E. Kristensson, A. Ehn, M. Aldén, J. Bood, *Opt. Lett.* 40 (2015) 5019–5022.
- [17] E. Berrocal, E. Kristensson, M. Richter, M. Linne, M. Alden, *Opt. Express* 16 (2008) 17870–17881.
- [18] M. Lewander, Z.G. Guan, K. Svanberg, S. Svanberg, T. Svensson, *Opt. Express* 17 (2009) 10849–10863.
- [19] T.L. Williams, *The Optical Transfer Function of Imaging Systems*, Institute of Physics, Bristol and Philadelphia, 1988.